



# AperTO - Archivio Istituzionale Open Access dell'Università di Torino

# The free energy density of a crystal: calcite (CaCO3) as a case of study

This is the author's manuscript	
Original Citation:	
Availability:	
This version is available http://hdl.handle.net/2318/154035	since 2016-06-16T15:23:14Z
Published version:	
DOI:10.1039/c4ce02203c	
Terms of use:	
Open Access	
Anyone can freely access the full text of works made available as under a Creative Commons license can be used according to the	
of all other works requires consent of the right holder (author or	
protection by the applicable law.	

(Article begins on next page)



# UNIVERSITÀ DEGLI STUDI DI TORINO

This is an author version of the contribution published on:

# BRUNO M.

The free energy density of a crystal: calcite (CaCO3) as a case of study CRYSTENGCOMM (2015)
DOI: 10.1039/C4CE02203C

The definitive version is available at: http://xlink.rsc.org/?DOI=C4CE02203C

The free energy density of a crystal: calcite (CaCO<sub>3</sub>) as a case of study

**BRUNO Marco\*** 

Dipartimento di Scienze della Terra, Università degli Studi di Torino, Via Valperga Caluso 35, I-

10125, Italy

\*Corresponding author

e-mail: marco.bruno@unito.it

Tel. +390116705126

Fax: +390116705128

Abstract

A new calculation methodology for determining the static energy density at 0K of each layer

forming the slab (i.e., how the static energy density varies within the slab) is proposed. This work is

the continuation of a previous one in which the vibrational free energy density of a slab was

estimated. Now, it becomes possible to determine the free energy density profile of a slab delimited

by any (hkl) surface and temperature, by adding the static contribution to the vibrational one.

Moreover, it is now possible to estimate the surface free energy of a crystal face without calculating

the free energy of the bulk. Finally, this model can be extended to the calculation of the free energy

of the interface between (i) two identical crystals in a twinning relationship and (ii) two different

crystals in an epitaxial relationship.

The model was applied to the (10.4) (twinned and untwinned), (10.0) and (01.2) slabs of calcite

(CaCO<sub>3</sub>): their free energy density profiles were calculated, as well as their surface/interface free

energies. At the best of my knowledge, this is the first time that it is evaluated how a planar defect

like a surface/interface affects the thermodynamic behavior of the underlying layers forming the

crystal.

**Keywords**: Free energy density, surface free energy, static energy, slab model, crystal surface

1

#### 1. Introduction

The study of the crystal surfaces (e.g., surface structure, adsorption phenomena, epitaxy, surface energy) is generally considered unconnected to that of the crystal bulk. The surface is usually interpreted as a sudden interruption of the bulk that does not generate particular repercussions on the thermodynamic and structural properties of the inner crystal. This point of view is likely the consequence of two factors: (i) a lacking of interest for this argument on the part of surface's scientists and (ii) the inability to determine how the main thermodynamic quantities (i.e., free energy, entropy, static energy), which describe the state of the system, vary from surface to bulk of the crystal. As concerns point (i) I am not able to intervene, while a contribution to the solution of the problem (ii) is furnished in this paper. To date, a first contribution to this item was recently given by Bruno and Prencipe, which conceived a new calculation methodology for determining the vibrational contribution of each layer forming the slab (i.e., how the vibrational free energy density at the temperature T varies within the slab), where the latter is a slice of crystal delimited by two parallel (hkl) faces. Their model uses the frequencies of the vibrational modes of a slab and it is based on the construction of a weight function taking into account how the vibrational amplitude of the atoms involved in the vibrational mode is modified by the presence of the surface.

The natural evolution of that work consists in the determination of the *static energy contribution at 0K* of each layer forming the slab (i.e., potential energy density profile) to add to the vibrational one for obtaining the Helmholtz free energy density profile. Therefore, in the present work I aim at determining the free energy density of a finite crystal, that is the Helmholtz free energy per volume unit (J m<sup>-3</sup>) of a crystalline phase delimited by {hkl} forms. I expect a strong variation of this thermodynamic quantity when moving from a (hkl) free surface to the center (bulk) of the crystal. Not only, a peculiar behavior of the free energy density should arise in proximity of each of the different (hkl) surfaces delimiting the crystal. As such modification is likely to be produced in the layers which are closer to the free surface, with respect to those more deeply buried in the crystal, it is interesting to analyze the contribution of the various layers to this quantity, as a function of the distance of each of them from the surface. For doing this, a new calculation methodology for determining the static energy density profile of a slab is proposed, which permits, by combining it with the one developed by Bruno and Prencipe<sup>1</sup> for the vibrational contribution, to study how the free energy density varies inside a crystal.

Moreover, by means of this new calculation methodology, it becomes possible to estimate the *surface free energy* of a (hkl) crystal face ( $\gamma^T_{(hkl)}$ ) at the temperature T of interest without calculating the free energy of the bulk. Furthermore, the calculation strategy here reported can be

extended to the study of the interface between (i) two identical crystals in twinning relationship, and (ii) two different crystals in epitaxial relationship.

Finally, in order to test the validity of the model, the free energy density profiles across the (10.4), (10.0) and (01.2) slabs of calcite (CaCO<sub>3</sub>) are determined and discussed, as well as the free energy density profile of the (10.4) twinned slab. I decided to study the (10.4), (10.0) and (01.2) faces because they are the main ones entering the equilibrium and growth shapes of calcite.<sup>2-4</sup> At the best of my knowledge, this is the first time that it is evaluated in a quantitative way how the crystal surfaces modify all of the thermodynamic properties of the bulk. That is, how a planar defect like a surface/interface affects the thermodynamic behaviour of the underlying layers forming the crystal.

# 2. Free energy density of a crystal

In order to determine the free energy density profile of a crystal, it is necessary to use the well known *slab model*, where a 2D periodic structure (slab) is generated by cutting the bulk crystal parallel to the *hkl* plane of interest. In this manner one is able to create a portion of the crystal having the thickness and surface termination desired, and obtain the Helmholtz free energy density associated to each layer of a *n*-layer slab,  $A_j$  (j = 1, ..., n). Obviously, to acquire a 3D picture of the free energy density of a crystal, several slabs with different (*hkl*) terminations must be taken into account. But before to describe the calculation strategy to employ for determining  $A_j$ , it is fundamental to highlight the following points:

(i)  $A_j$  (J m<sup>-3</sup>) is the sum of two terms (both referred to the *j*-th layer):

$$A_{j} = E_{j}^{0} + A_{j}^{vib}$$
 (1)

where  $E_j^0$  (J m<sup>-3</sup>) is the static energy density at 0K and  $A_j^{vib} = E_j^{vib} - TS_j^{vib}$  is the vibrational free energy density at the temperature T of interest;  $E_j^{vib}$  (J m<sup>-3</sup>) and  $S_j^{vib}$  (J m<sup>-3</sup> K<sup>-1</sup>) are the vibrational energy density (including the zero point energy) and vibrational entropy density, respectively, at the temperature T (K).

- (ii) The slab is composed by n-layer, each one with thickness  $d_{hkl}$  (interplanar distance: the distance between adjacent hkl planes).
- (iii)  $E_j^0$  can be determined by using several codes developed for performing empirical (i.e., GULP,<sup>5</sup> TINKER<sup>6</sup>), semi-empirical (i.e., MOPAC<sup>7</sup>) and *ab initio* quantum-mechanical (i.e., ABINIT,<sup>8,9</sup> CASTEP,<sup>10</sup> CRYSTAL,<sup>11</sup> Quantum ESPRESSO,<sup>12</sup> VASP<sup>13</sup>) calculations on crystalline materials.

(iv) Instead, as detailed in a later paragraph, the estimate of  $A_j^{vib}$  requires the use of two computational codes in sequence: (a) initially, a code (GULP or CRYSTAL) for the calculation of the frequencies of the vibrational modes of a slab; (b) successively, the SLAB code, which reads the output files generated by GULP or CRYSTAL and computes  $A_i^{vib}$  by means of the relations reported in the paragraph 2.2.

#### FIGURE 1

#### 2.1. Static energy density

For determining the static energy density of a slab at 0K,  $E_j^0$  (J m<sup>-3</sup>), a remarkable number of calculations have to be performed. In order to detail the calculation procedure, the sequence of operations to perform is listed below:

- (i) First of all, it is needed to optimize the structure of the n-layer slab delimited by the (hkl) faces of interest (Fig. 1a). As a consequence, a static energy  $E^0$  results to be associated to the optimized slab. Usually, the calculation programs express  $E^0$  as J/(z f.u.), where z is the number of formula units (f.u.) forming the slab. But, for convenience, one converts this unit of measurement in J m<sup>-3</sup>, multiplying  $E^0$  by the factor  $N_A \rho/(zM_W)$ , where  $N_A$  is the Avogadro's number,  $\rho$  is the density of the phase (kg m<sup>-3</sup>) and  $M_W$  is the molecular weight of a f.u. (kg mol<sup>-1</sup>).
- (ii) Then, one isolates the *j*-th layer (j = 1,..., n) from the optimized slab and calculates its static energy  $(E_j)$ ; this calculation must be performed for each layer forming the slab (Fig. 1b). As in the case of  $E^0$ , one multiplies  $E_j$  by  $N_A \rho/(tM_W)$  for converting the energy term from J/(t f.u.) to  $J \text{ m}^{-3}$ , where t is the number of f.u. forming the layer.
- (iii) Successively, one isolates the couple of layers from the optimized slab with indexes j=1,...,n-1 and i=j+1 (Fig. 1c), and calculates its static energy ( $E_{j,i}$ ). Also in this case, one multiplies  $E_{j,i}$  by  $N_A \rho/(tM_W)$  for having the energy term in J m<sup>-3</sup>. This procedure must be carried out for all of the couples of layers forming the slab: for a n-layer slab the number of couples to consider is given by  $\sum_{i=1}^{n-1} (n-i)$ . Overall, by also considering the points (i) and
  - (ii), the number of calculations to perform is  $n+1+\sum_{i=1}^{n-1} (n-i)$ .

(iv) Finally, one is able to calculate the static energy density at 0K of the j-th layer included in the optimized slab ( $E_j^0$ ), by taking into account its interaction energy with all of the others layers, by means of the equation:

$$E_{j}^{0} = E_{j} + \frac{1}{2} \sum_{i=j+1}^{n} \left[ E_{j,i} - \left( E_{j} + E_{i} \right) \right]$$
 (2)

 $E_j^0$  describes how the static energy density varies across a slab, from the surface layers to the bulk ones (i.e., the layers at the center of the slab).

For a thick slab, the number of calculations could be drastically reduced by verifying when the term  $E_{1,i} - (E_1 - E_i)$  approaches to zero with the increase of the index i. Indeed, if one finds that this difference is close to zero, e.g., for the layer having index i = 4, then it is sufficient to determine the contributions  $E_{j,j+1}$ ,  $E_{j,j+2}$  and  $E_{j,j+3}$  for j = 1, ..., n-1.

### 2.2. Vibrational free energy density

The strategy and equations for determining the vibrational contribution of each layer or atom forming a slab were described in a recent paper by Bruno and Prencipe. Therefore, in the present work I only detail the operating procedure to follow for calculating  $A_j^{vib}$ . A two-step procedure can be envisaged:

- (i) By using GULP or CRYSTAL, one computes for the optimized slab the frequencies (eigenvalues) of the vibrational modes and the eigenvectors of the mass weighted Hessian matrix describing the vibrational modes, which are listed in an output file.
- (ii) Successively, the SLAB program reads the frequencies and eigenvectors from the output file created by GULP or CRYSTAL, and calculates the thermodynamic quantity  $E_j^{vib}$ ,  $S_j^{vib}$  and  $A_j^{vib}$  for each layer forming the slab (j=1,...,n). Since SLAB gives the values of energy ( $E_j^{vib}$  and  $A_j^{vib}$ ) and entropy  $S_j^{vib}$  in J (and J K<sup>-1</sup>) per mole of z f.u., it is necessary to multiply them by  $\rho/(tM_W)$  for having J m<sup>-3</sup> and J m<sup>-3</sup> K<sup>-1</sup>.

# 3. Application of the model to the (10.4), (10.0) and (01.2) faces of calcite

Structure optimization and calculation of the vibrational frequencies of the (10.4), (10.0) and (01.2) slabs of calcite were performed at empirical level by using the calcite force field developed by Rohl

et al.<sup>14</sup> and the version 4.0 of the GULP simulation code.<sup>5</sup> The Rohl's force field very successfully reproduced the equilibrium geometries and the surface energy values at T = 0K of the {10.4} and {01.2} faces obtained from *ab initio* calculations at DFT (Density Functional Theory; B3LYP<sup>15</sup> and PBE<sup>16</sup> Hamiltonians) level,<sup>17-19</sup> as well as the experimental observations of the surface relaxation of the {10.4} form.<sup>14</sup> A detailed discussion on the ability of the Rohl potential<sup>14</sup> to reproduce the surface energy values of the crystal faces discussed in this work is reported in the paper by Bruno et al.<sup>2</sup> In the same paper,<sup>2</sup> the comparison between experimental and theoretical determinations of the surface energy of the main crystal faces of calcite is also done. Furthermore, a fairly good agreement exists between the twinning energies of the four twin laws of calcite calculated with the Rohl potential<sup>20</sup> and those determined at DFT level.<sup>21</sup>

The geometry optimization was performed by considering (10.4), (10.0) and (01.2) slabs formed by 10, 15 and 12 layers, respectively; the number of f.u. (zCaCO<sub>3</sub>) forming the (10.4), (10.0) and (01.2) slabs is 60, 90 and 72, respectively. These thicknesses are sufficient to satisfy the criterion of convergence, that is the bulk-like properties are reproduced at the center of the slab. The center of inversion was retained in the calculations, to ensure that the dipole moment perpendicular to the slab was equal to zero.

The vibrational thermodynamic properties were calculated at T = 298.15K. The frequencies of the vibrational modes of the (10.4), (10.0) and (01.2) slabs were calculated by considering 30 k points. As discussed later, this number of k points is sufficient to obtain a reliable estimate of the vibrational thermodynamic quantities.

#### FIGURE 2

#### 3.1. (10.4) face

In Fig. 2 (left column) the quantities  $A_j$ ,  $E_j^0$  and  $A_j^{vib}$  are plotted; their numerical values, along with those of  $E_j^{vib}$  and  $S_j^{vib}$ , are listed in Table S1 (ESI). By analyzing Fig. 2, one observes an abrupt decrease of  $A_j$  and  $E_j^0$  moving from the surface (layers 1 and 10) toward the center of the slab, whereas  $A_j^{vib}$  shows an opposite behavior, it increases from the surface to the center of the slab. Moreover, it is interesting to note that:

(i) all of these quantities converge very quickly to their bulk value. Indeed, only the thermodynamic values of the layers j = 1, 2 and 3 show significant differences with respect to those at the center of the slab (i.e., bulk values); in particular, it is the layer 1 (or its

equivalent: layer 10) to show the highest variation. This put in evidence that the thickness of the crystal mainly interested by the perturbation generated by the presence of the (10.4) surface, is  $\sim 10$  Å.

- (ii) The contribution of  $A_j^{vib}$  to  $A_j$  is always < 1% (Table S1 in ESI): 0.78% for the layer 1 (and 10) and 0.85% for all others ones. This reveals that for the (10.4) slab the vibrational contribution is higher for the bulk than for the surface.
- (iii) At 298.15K, one observes that for each layer  $\left|E_{j}^{vib}\right|$  is about twofold the term  $\left|TS_{j}^{vib}\right|$ . Such a relation is valid also for the (10.0) and (01.2) slabs analyzed in the following paragraphs.

Now, one is able to calculate the surface free energy at 298.15K of the (10.4) face, ( $\gamma_{(10.4)}^{298.15}$ ; the specific Helmholtz free energy needed for the creation of a crystal surface at the temperature T of interest), by using the equation proposed by Bruno and Prencipe:<sup>1</sup>

$$\gamma_{(10.4)}^{298.15} = \left[ \left( \sum_{j=1}^{n} A_j \right) - n A_{n/2} \right] \frac{d_{10.4}}{2}$$
 (3)

The term inside the square bracket is the difference between the free energy of the slab (with n=10) and that of the bulk: indeed,  $A_{n/2}$  is the free energy value at the center of the slab, representing the bulk value (i.e., in this case  $A_{n/2}=A_5$ );  $d_{10.4}=3.0338\times10^{-10}$  m; 2 accounts for the existence of two surfaces delimiting the slab. According to eq. 3,  $\gamma_{(10.4)}^{298.15}$  results to be 0.499 J m<sup>-2</sup> (Table 1).

Furthermore, always according to the work by Bruno and Prencipe,  $^1$  it is licit to write  $\gamma_{(10.4)}^{298.15}$  as the sum of two terms:

$$\gamma_{(10.4)}^{298.15} = \gamma_{(10.4)}^{0} + \gamma_{(10.4)}^{298.15,vib}$$
 (4)

where  $\gamma^0_{(10.4)}$  is the surface energy at T=0K (the specific work needed for creating and relaxing a crystal face at 0K and without considering vibrational zero point effects);  $\gamma^{298.15,vib}_{(10.4)}$  is the vibrational (thermal) contribution (the specific internal vibrational energy and vibrational entropy at the temperature T, including the zero point energy contribution).  $\gamma^0_{(10.4)}$  and  $\gamma^{298.15,vib}_{(10.4)}$  can be calculated by inserting  $E^0_j$  ( $E^0_5$ ) and  $A^{vib}_j$  ( $A^{vib}_5$ ) in eq. 3, respectively, at the place of  $A_j$ : 0.499 and -0.027 J

m<sup>-2</sup> are the resulting values (Table 1). As expected, the contribution of  $\gamma_{(10.4)}^{298.15,vib}$  to  $\gamma_{(10.4)}^{298.15}$  is very low, ~5%;  $\gamma_{(10.4)}^{0}$  is poorly modified at room temperature by vibrational contributions.

In order to verify the criterion of convergence, the estimate of  $\gamma_{(10.4)}^{298.14,vib}$  calculated for the 10-layer slab and with 30 k points can be compared with the value (-0.030 J m<sup>-2</sup>) obtained in a previous work,<sup>2</sup> where the (10.4) slab and bulk entropy of calcite at T = 300K were determined, by means of another calculation method and respecting the convergence criteria on the number of k points and slab thickness, but always using the Rohl's potential and GULP simulation code. The good agreement between these two independent estimates, is guarantee of adequacy on the number of k points adopted in this work.

**Table 1.** Surface energy at 0K ( $\gamma_{(hkl)}^0$ ), and surface free energy ( $\gamma_{(hkl)}^{298.15}$ ) and surface vibrational energy at 298.15K ( $\gamma_{(hkl)}^{298.15,vib}$ ) of the (10.4), (10.0) and (01.2) faces of calcite; all of these quantities are expressed in J m<sup>-2</sup>. The percentage contribution of  $\gamma_{(hkl)}^{298.15,vib}$  to  $\gamma_{(hkl)}^{298.15}$  is also reported,  $\Delta(\%) = \left|\gamma_{(hkl)}^{298.15,vib} / \gamma_{(hkl)}^{298.15} \right| \times 100$ .

face	$\gamma_{(hkl)}^{298.15}$	$\gamma^0_{(hkl)}$	$\gamma_{(hkl)}^{298.15,vib}$	Δ(%)
(10.4)	0.499	0.526	-0.027	5.1
(10.0)	0.725	0.719	0.006	0.8
(01.2)	0.736	0.738	-0.002	0.3

# 3.2. (10.0) face

In Fig. 3 (left)  $A_j$ ,  $E_j^0$  and  $A_j^{vib}$  are plotted; their numerical values, along with those of  $E_j^{vib}$  and  $S_j^{vib}$ , are listed in Table S2 (ESI). For a detailed description of the (10.0) surface structure, see the paper by Massaro et al.<sup>22</sup>

As for the (10.4) face, one observes an abrupt decrease of  $A_j$  and  $E_j^0$  moving from the surface (layers 1 and 15) toward the center of the slab (layer 8), whereas a totally different behavior of  $A_j^{vib}$  is registered, whose more evident features are: (i) the highest and lowest values placed in correspondence of layers 1 and 2, respectively, and (ii) a surface value ( $A_1^{vib}$ ) higher than the bulk one ( $A_8^{vib}$ ). Also for the (10.0) face, it is interesting to underline:

- (i) a very rapid convergence of  $A_j$ ,  $E_j^0$  and  $A_j^{vib}$  to their bulk values, since only the thermodynamic values related to layers j=1, 2 and 3 show significant differences with respect to those at the center of the slab. As a consequence, a thickness of ~ 13 Å results to be perturbed by the presence of the (10.0) surface.
- (ii) The contribution of  $A_j^{vib}$  to  $A_j$  is always < 1% (Table S2 in ESI), but in this case the importance of the vibrational term is greater for surface layer (1 or 15), 0.88%, than for the bulk (layer 8), 0.85%.

By inserting in eq. 3 the quantities related to the (10.0) slab ( $E_8^0$ ,  $A_8^{vib}$ ,  $A_8$ , n=15,  $d_{10.0}=4.3140\times10^{-10}$  m), one obtains  $\gamma_{(10.0)}^{298.15}$ ,  $\gamma_{(10.0)}^0$ , and  $\gamma_{(10.0)}^{298.15,vib}$ , whose values are listed in Table 1. The low and positive value of  $\gamma_{(10.0)}^{298.15,vib}$  (0.006 J m<sup>-2</sup>) is likely of the order of magnitude of the numerical error that affects the calculations, therefore one can consider negligible the vibrational contribution to the surface free energy of the (10.0) face.

#### 3.3. (01.2) face

In Fig. 3 (right) and Table S2 (ESI), the thermodynamic quantities  $A_j$ ,  $E_j^0$  and  $A_j^{vib}$  of the (01.2) face are reported; the (01.2) surface structure is described in the paper by Bruno et al.<sup>17</sup>

The main feature of the (01.2) slab concerns the behavior of  $A_j^{vib}$ : the surface (layers 1 and 12) and bulk (layer 6) show similar values of  $A_j^{vib}$ , whereas the layer 2 (and 11) displays the lowest one. Instead, the functions  $A_j$  and  $E_j^0$  show a trend similar to that previously described for the (10.4) and (10.0) slabs, as well as the slab thickness altered by the (01.2) surface ( $\sim$  12 Å).

The thermodynamic surface quantities of the (01.2) face (calculated with:  $E_6^0$ ,  $A_6^{vib}$ ,  $A_6$ , n=12,  $d_{01.2}=3.8501\times10^{-10}$  m) have strong analogies with those of the (10.0) one (Table S2 in ESI). In particular, the value of  $\gamma_{(01.2)}^{298.15,vib}$  (-0.002 J m<sup>-2</sup>) is negligible when compared to that of  $\gamma_{(01.2)}^0$  (0.738 J m<sup>-2</sup>).

#### 4. Application of the model to the (10.4) twinned calcite

Structure optimization and calculation of the vibrational frequencies of the (10.4) twinned slab of calcite were performed by using the Rohl's force field<sup>14</sup> and GULP.<sup>5</sup>

A twinned slab, made by slabs A and B, was generated in the following way: (i) the slab A of a given thickness was made by cutting the bulk structure parallel to the *hkl* twin plane of interest; (ii) the slab B was made by applying the appropriate twin law (i.e, a mirror plane parallel to 10.4) to

the atomic coordinates of the slab A; (iii) then, the twinned slab geometry (atomic coordinates) was optimized by considering all the atoms free to move. For more details on the construction of the twinned slab see the paper by Bruno et al.<sup>20</sup>

The calculations were performed at T = 298.15K by considering the (10.4) twinned slab formed by 24 layers (12 layers both for A and B) and 144 f.u. (zCaCO<sub>3</sub>). The frequencies of the vibrational modes of the (10.4) twinned slab were calculated by considering only 2 k points. The thickness and the number of k points are not sufficient to satisfy the criterion of convergence, that is the bulk-like properties are not reproduced at the center of the slabs A and B. Unfortunately, at the time being, I am not able to take into account a thicker slab and more k points. This restriction is due to the fact that one must read the eigenvectors (representing the normal modes) from the output file of GULP, which is enormous (and as a consequence, it is not manageable) when a high number of atoms and k points is used. Therefore, in order to reach convergence, it should be necessary to implement the calculation strategy in the GULP code. Nevertheless, a reliable estimate of the thermodynamic properties of the twinned slab was obtained.

 $A_j$ ,  $E_j^0$  and  $A_j^{vib}$  are plotted in Fig. 1 (right), whereas their numerical values are listed in Table S1 (ESI). The existence of the (10.4) twinned interface generates an oscillation of the thermodynamic functions that propagates throughout the whole slab. This is a clear evidence that the slab thickness used to model the twinned crystal is not sufficient for reproducing the bulk properties at the center of the slabs A and B. Despite that, an evident increment of  $A_j$  is identifiable at the surface (layers 1 and 24) and at the twinned interface (layers 12 and 13). As well as it is interesting to note that, at variance with the free surface, an increase of  $A_j^{vib}$  is detected in the layers forming the twinned interface.

A fundamental thermodynamic quantity related to a twinned slab is the twinning free energy  $(\gamma_{TE}^{298.15}; \text{ J m}^{-2})$ , which is the excess free energy required to form a unit area of the twin boundary interface at the temperature T of interest (i.e., 298.15K). It can be calculated with the following relation, developed by Bruno and Prencipe<sup>1</sup> and adapted in this work to the studied case:

$$\gamma_{TE}^{298.15} = \left[ \left( \sum_{j=6}^{19} A_j \right) - 6A_6 \right] d_{10.4}$$
 (5)

which gives  $\gamma_{TE}^{298.15} = 0.252$  J m<sup>-2</sup>. In analogy with the surface free energy, it is possible to write  $\gamma_{TE}^{298.15}$  as the sum of two terms:

$$\gamma_{TE}^{298.15} = \gamma_{TE}^{0} + \gamma_{TE}^{298.15,vib} \quad (6)$$

where  $\gamma_{TE}^0$  is the excess static energy at 0K required to form a unit area of the twin boundary interface and  $\gamma_{TE}^{298.15,vib}$  is the vibrational contribution of the twin boundary interface at T=298.15K. By inserting  $E_j^0$  ( $E_6^0$ ) and  $A_j^{vib}$  ( $A_6^{vib}$ ) in eq. 5 at the place of  $A_j$  ( $A_6$ ), one obtains  $\gamma_{TE}^0=0.234$  and  $\gamma_{TE}^{298.15,vib}=0.018$  J m<sup>-2</sup>. At variance with the (10.4) surface free energy, the vibrational contribution tends to increase the value of  $\gamma_{TE}^0$ .

#### FIGURE 3

#### 5. Conclusions

In this paper a calculation methodology for determining the static energy density at 0K of each layer forming the slab (i.e., how the static energy density varies within the slab) is described. This work is the continuation of a previous one<sup>1</sup> in which the vibrational free energy density of a slab was estimated. Now, by putting together the static and vibrational contributions, it becomes possible to determine the free energy density profile of a slab delimited by any (hkl) surface and temperature. Moreover, it is now possible to estimate the surface free energy of a crystal face ( $\gamma_{(hkl)}^T$ ) without calculating the free energy of the bulk. Finally, this model can be extended to the calculation of the free energy of the interface between (i) two identical crystals in a twinning relationship and (ii) two different crystals in an epitaxial relationship.

In order to test the model, the following systems were studied: (i) surfaces: 10-layer (10.4), 15-layer (10.0) and 12-layer (01.2) slabs of calcite (CaCO<sub>3</sub>); (ii) interface: 24-layer (10.4) twinned slab of calcite. In all of these cases, the static energy, vibrational energy, vibrational entropy, vibrational free energy and free energy of the optimized slab, and the contribution to these quantities of each layer forming the slab were calculated; the vibrational contribution were determined at T = 298.15K. Then, the surface free energy at 298.15K of the (10.4), (10.0) and (01.2) faces were evaluated, as well as the twinning free energy of the (10.4) twinned slab. At my knowledge, this is the first time that a complete thermodynamic analysis of a crystal and its main faces was performed. In particular, it is the first time that the effect of the surfaces on the thermodynamic behaviour of the underlying layers forming the crystal is evaluated in a quantitative way.

Another interesting application of the present model concerns the study of the interface between two different phases in epitaxial relationship. The calculation methodology to apply for such a system is the same adopted for the twinned slab described in this paper. The only difference consists in having a slab made up of two portions with different chemical composition at the place of two portions with the same one. The determination of its free energy density profile could give new and interesting ideas to explain the origin of the epitaxy from a thermodynamic point of view. Then, since the epitaxy is a fundamental phenomenon usually observed during nucleation and growth of electronic materials above crystalline templates, the calculation method proposed in this work could be a valid instrument to gain more insights on its formation mechanisms.

At present the calculation methodology described in this work for determining the static energy density, is not implemented in a computational code. It requires a remarkable number of calculations, which can become prohibitive when a large system with a complex stoichiometry is analyzed at quantum-mechanical level. A possible way to reduce drastically the number of calculations could consist in the identification of a *weight function* relating the contribution of each layer to the static energy of a slab with a suitable parameter that describes the evolution of the slab structure from its surface to bulk (e.g., variation of  $d_{hkl}$  across the slab). But for identifying a similar weight function, it is necessary to perform a detailed structural analysis of the slab and to build tentatively the structural parameter that fits better the behavior of the static energy density profile, as determined with the strategy employed in this work. Then, a future development of the present work can concern the creation of this weight function.

A further progression, on which I am already working, concerns the conception of a analytical model for the determination of the thermodynamic properties of the crystal/aqueous solution interface. By describing the crystal with the present model and doing some assumptions on the behavior of the fluid in proximity of the crystal surface, one will be able to estimate the free energy of the crystal/solution interface at whatever temperature, a crucial quantity to estimate the probability of nucleation of a phase and, then, to observe it in laboratory or Nature.

#### Acknowledgements

Thanks are due to two anonymous reviewers for their careful reading of the manuscript and their fundamental observations on our work.

#### References

- 1 M. Bruno and M. Prencipe, *CrystEngComm*, 2013, **15**, 6736-6744.
- 2 M. Bruno, F. R. Massaro, L. Pastero, E. Costa, M. Rubbo, M. Prencipe and D. Aquilano, *Crystal Growth & Design*, 2013, **13**, 1170-1179.

- 3 D. Aquilano, M. Bruno, F. R. Massaro and M. Rubbo, *Crystal Growth & Design*, 2011, **11**, 3985-3993.
- 4 F. R. Massaro, M. Bruno, D. Aquilano, Crystal Growth & Design, 2010, 10, 4096-4100.
- 5 J. D. Gale, J. Chem. Soc. Faraday Trans., 1997, 93, 629-637.
- 6 J. W. Ponder, Tinker, Software Tools for Molecular Design, Version 6.0, June 2011.
- 7 J. P. James, MOPAC2012, Stewart, Stewart Computational Chemistry, Colorado Springs, CO, USA, 2012, <a href="http://OpenMOPAC.net">http://OpenMOPAC.net</a>.
- 8 X. Gonze, B. Amadon, P.-M. Anglade, J.-M. Beuken, F. Bottin, P. Boulanger, F. Bruneval, D. Caliste, R. Caracas, M. Cote, T. Deutsch, L. Genovese, Ph. Ghosez, M. Giantomassi, S. Goedecker, D. R. Hamann, P. Hermet, F. Jollet, G. Jomard, S. Leroux, M. Mancini, S. Mazevet, M. J. T. Oliveira, G. Onida, Y. Pouillon, T. Rangel, G.-M. Rignanese, D. Sangalli, R. Shaltaf, M. Torrent, M. J. Verstraete, G. Zerah and J.W. Zwanziger, *Computer Phys. Commun.*, 2009, **180**, 2582-2615.
- 9 X. Gonze, G.-M. Rignanese, M. Verstraete, J.-M. Beuken, Y. Pouillon, R. Caracas, F. Jollet, M. Torrent, G. Zerah, M. Mikami, Ph. Ghosez, M. Veithen, J.-Y. Raty, V. Olevano, F. Bruneval, L. Reining, R. Godby, G. Onida, D. R. Hamann, and D. C. Allan, *Zeit. Kristallogr.*, 2005, **220**, 558-562.
- 10 M. D. Segall, P. L. D. Lindan, M. J. Probert, C. J. Pickard, P. J. Hasnip, S. J. Clark, and M. C. Payne, *J. Phys.: Condens. Matter*, 2002, **14**, 2717-2744.
- 11 R. Dovesi, V. R. Saunders, C. Roetti, R. C. Orlando, M. Zicovich-Wilson, F. Pascale, B. Civalleri, K. Doll, N.M. Harrison, I.J. Bush, Ph. D'Arco, and M. Llunell, *CRYSTAL09 User's Manual*, University of Torino, Torino, 2013.
- 12 P. Giannozzi, S. Baroni, N. Bonini, M. Calandra, R. Car, C. Cavazzoni, D. Ceresoli, G. L. Chiarotti, M. Cococcioni, I. Dabo, A. Dal Corso, S. de Gironcoli, S. Fabris, G. Fratesi, R. Gebauer, U. Gerstmann, C. Gougoussis, A. Kokalj, M. Lazzeri, L. Martin-Samos, N. Marzari, F. Mauri, R. Mazzarello, S. Paolini, A. Pasquarello, L. Paulatto, C. Sbraccia, S. Scandolo, G. Sclauzero, A. P. Seitsonen, A. Smogunov, P. Umari and R. M. Wentzcovitch, *J. Phys.: Condens. Matter*, 2009, **21**, 395502.
- 13 G. Kresse, M. Marsman and J. Furthmüller, VASP Manual, University of Vienna, Vienna, 2012.
- 14 A. L. Rohl, K. Wright and J. D. Gale, Am. Miner., 2003, 88, 921-925.
- 15 A. D. Becke, J. Chem. Phys., 1993, 98, 5648-5652.
- 16 J. P. Perdew, K. Burke and M. Ernzerhof, *Phys. Rev. Lett.*, 1996, **77**, 3865-3868.
- 17 M. Bruno, F. R. Massaro and M. Prencipe, Surf. Sci., 2008, 602, 2774-2782.
- 18 M. Bruno, F. R. Massaro, M. Prencipe and D. Aquilano, CrystEngComm, 2010, 12, 3626-3633.
- 19 T. Akiyama, K. Nakamura and T. Ito, Physical Review B, 2011, 84, 085428.
- 20 M. Bruno, F. R. Massaro, M. Rubbo, M. Prencipe and D. Aquilano, *Crystal Growth & Design*, 2010, **10**, 3102-3109.
- 21 T. Akiyama, K. Nakamura and T. Ito, *The Journal of Physical Chemistry C*, 2012, **116**, 987-993.
- 22 F. R. Massaro, M. Bruno and D. Aquilano, Crystal Growth & Design, 2010, 10, 4096-4100.

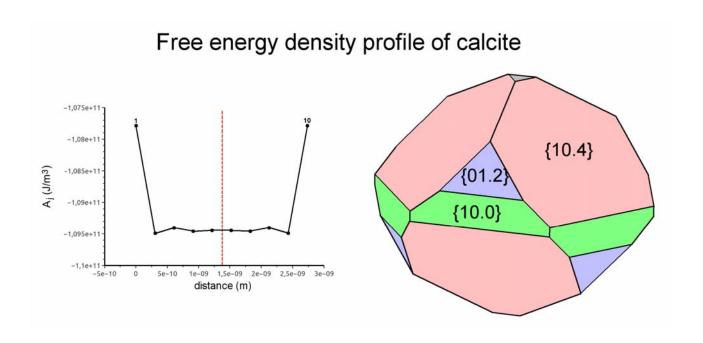
#### Figure captions

**Figure 1.** Graphical representation of the calculation sequence to perform for determining  $E_j^0$ . (a) Optimization of the structure of the *n*-layer slab: in this way a static energy at 0K equal to  $E^0$  is obtained; (b) extraction of the layer j=2 from the optimized slab and determination of its energy  $E_2$ ; (c) extraction of a couple of layers (j=2 and n) from the optimized slab and determination of its energy  $E_{2n}$ .

**Figure 2.** Free energy  $(A_j)$ , static energy  $(E_j^0)$  and vibrational free energy  $(A_j^{vib})$  density of the layers forming the (10.4) slab and (10.4) twinned slab of calcite; free energy and vibrational free energy were calculated at T = 298.15K. Each point in the graph represents a layer of the slab: only the numbers that identify the surface layers are reported; in the abscissa the distance between layer 1 (chosen as zero) and n is reported. The red dotted line shows the center of the slab.

**Figure 3.** Free energy  $(A_j)$ , static energy  $(E_j^0)$  and vibrational free energy  $(A_j^{vib})$  density of the layers forming the (10.4) and (01.2) slabs of calcite; free energy and vibrational free energy were calculated at T = 298.15K. Each point in the graph represents a layer of the slab: only the numbers that identify the surface layers are reported; in the abscissa the distance between layer 1 (chosen as zero) and n is reported. The red dotted line shows the center of the slab.

# **Graphical Abstract**



A new calculation methodology for determining the static energy density at 0K of each layer forming the slab (i.e., how the static energy density varies within the slab) is proposed. Now, it becomes possible to determine the free energy density profile of a slab delimited by any (*hkl*) surface and temperature.